Article published online: 2024-01-17

Identification of CT Features to Differentiate Pulmonary Sarcoma from Carcinoma

Supraja Laguduva Mohan[1] Ekta Dhamija[1] Sameer Bakhshi[2] Prabhat Singh Malik[2] Sameer Rastogi[2] Chandrashekhara Sheragaru Hanumanthappa[1] Deepali Jain[3] Rambha Pandey[4]

[1] Department of Radiodiagnosis, All India Institute of Medical Sciences, New Delhi, India
[2] Department of Medical Oncology, All India Institute of Medical Sciences, New Delhi, India
[3] Department of Pathology, All India Institute of Medical Sciences, New Delhi, India
[4] Department of Radiation Oncology, All India Institute of Medical Sciences, New Delhi, India

Address for correspondence Ekta Dhamija, MD, Department of Radiodiagnosis, All India Institute of Medical Sciences, Room number 137, First floor, New Delhi 110029, India (e-mail: drektadhamija.aiims@gmail.com).

Indian J Radiol Imaging 2024;34:390–404.

Abstract

Background Primary lung sarcoma (PLS) differs in management protocols and prognosis from the more common primary lung carcinoma (PLC). It becomes imperative to raise a high index of suspicion on radiological and pathological features.

Purpose The aim of this study is to highlight the variable imaging appearances of PLS compared with PLC, which impacts radiologic - pathologic correlation.

Materials and Methods A retrospective observational study of 68 patients with biopsy-proven lung tumors who underwent baseline imaging at our tertiary care cancer hospital was conducted between January 2018 and March 2022. The patient details and imaging parameters of the mass on contrast-enhanced computed tomography (CECT) were recorded and analyzed for patients with PLS and compared with PLC. Follow-up imaging was available in 9/12 PLS and 52/56 PLC patients.

Results Among 12 patients with PLS, 5 patients had synovial sarcoma on histopathology. PLS was seen in patients with a mean age of 40.8 years; the mass showed a mean size of 13.2 cm, lower lobe (75%), parahilar (75%), hilar involvement (41.7%), oval shape (41.7%), circumscribed (25%) or lobulated (75%) margins, lower mean postcontrast attenuation of 57.3 HU, fissural extension (50%), calcification (50%), and no organ metastasis other than to the lung. PLC (56 patients) was seen in the elderly with a mean age of 54.8 years; the mass showed a mean size of 5.7 cm, irregular shape (83.9%), spiculated margins (73.2%), higher mean postcontrast attenuation (77.3 HU), chest wall infiltration (30.4%), and distant metastasis (58.9%) at baseline imaging. A statistically significant difference ($p < 0.05$) was seen between sarcoma and carcinoma in the mean age, size, site, shape, margins, postcontrast attenuation, presence of calcifications, fissural extension, and distant metastasis.

Conclusion The distinct imaging features of sarcoma help in differentiating it from carcinoma. This can also be used to corroborate with histopathology to achieve concordance and guide clinicians on further approach.

Keywords
- lung neoplasms
- carcinoma
- sarcoma
- synovial sarcoma
- SYT–SSX fusion protein

article published online
January 17, 2024

DOI https://doi.org/10.1055/s-0043-1777834.
ISSN 0971-3026.

Thieme Medical and Scientific Publishers Pvt. Ltd., A-12, 2nd Floor, Sector 2, Noida-201301 UP, India

Introduction

According to Global Cancer Observatory's Online database (GLOBOCAN) 2020, lung cancer is the second most common malignancy in the world, accounting for 11.4% of all cancers and 18% of all cancer deaths. Most of the malignant lung neoplasms arise from the respiratory epithelium and are classified as adenocarcinoma, squamous cell carcinoma, small cell carcinoma, and large cell carcinoma, with incidences of 38.5, 20, 15, and 2.9%, respectively.[1,2] Thoracic sarcoma, on the other hand, is a rare tumor that can arise from the mesenchymal tissue in the mediastinum, pulmonary artery, chest wall, pleura, and the lung. The two entities differ in location, histology, microvascular architecture, and gross imaging appearance. The carcinomas arise from the epithelium with acinar structure or mucin production (adenocarcinoma), keratinization, or intercellular bridges (squamous cell carcinoma), with neuroendocrine cells in small cell carcinoma or without lineage-specific differentiation in large cell carcinoma.[3] Sarcomas, on the other hand, are comprised of mesenchymal tissue, which includes spindle cells, endothelial cells, perivascular cells, lymphatic vessels, myoepithelial cells, cartilage, and other connective tissue elements depending on their type.[4] While carcinomas contain bursts of clustered vessels as they usually contain vascular epithelial and less vascular benign stromal compartments, sarcomas are made up of malignant mesenchymal tissue alone and hence show homogeneously and diffusely distributed vessels.[5] Tumor microvessel density is higher for tumors with high metabolic demand, and it is highest in adenocarcinoma among lung carcinomas.[6,7] The different types of carcinoma and sarcoma show positivity to different immunohistochemistry markers and have specific molecular profiles. Owing to all these differences, they show different imaging features on contrast-enhanced computed tomography (CECT). The pathological types of sarcomas, which are commonly intrathoracic, include leiomyosarcoma or pulmonary intimal sarcoma (from the pulmonary artery intima), rhabdomyosarcoma, and angiosarcoma (cardiac), whereas Ewing's sarcoma, chondrosarcoma, and synovial sarcoma (SS) are commonly chest wall based.[8] The advances in molecular techniques have also led to the identification of a new distinct entity—*SMARCA4*-deficient undifferentiated tumor or *SMARCA4*-deficient thoracic sarcoma (*SMARCA4*–DTS), which is included in the fifth edition of the WHO classification for lung tumors.[9] Treatment strategies for carcinoma include anatomical resection (segmentectomy or lobectomy), cisplatin-based chemotherapy regimens, driver mutation-guided tyrosine kinase inhibitors (TKIs), immunotherapy (PD–L1 inhibitors), stereotactic radiotherapy, and radiofrequency ablation, with standard therapy regimens based on their stage.[10] For sarcoma, due to its rarity, there is no standard treatment regimen. Combinations of surgical nonanatomical resection, radiotherapy, and different chemotherapy and targeted agents are tailored to the specific type of sarcoma.[11] The 5-year survival rate for lung carcinomas is 10 to 20% and that for lung sarcoma is 44 to 48%.[12–14] Despite these differences, a differential diagnosis of pulmonary sarcoma is seldom considered before histopathological assessment due to limited available literature comparing the imaging features of sarcoma and carcinoma. This study attempts to characterize and differentiate the imaging features of primary lung sarcoma (PLS) from primary lung carcinoma (PLC), which can help in clinical and pathological correlation and follow-up.

Materials and Methods

Study Population

This retrospective study was conducted in the department of radiology of a dedicated tertiary care cancer hospital (single center), after obtaining approval from the institute's ethics committee (IEC-576/15.07.2022) and in view of the retrospective nature of the study, individual informed consent was waived off. The reporting database was searched for patients with proven malignancies of lung who underwent imaging evaluation at our institute between January 2018 and March 2022. Lung masses in adults (>18 years) with histopathological diagnosis of lung tumors with or without metastasis, who had at least one baseline CECT imaging done in our institute, were included.

Clinical Assessment

The demographic, clinical, and pathological details were obtained from the institutional case records. Histopathological diagnosis was considered the gold standard. Clinical data including history of smoking and date of diagnosis of PLS/PLC and metastases were recorded.

Imaging Acquisition

As per the institute's policy, we performed a single-phase CECT for patients with lung masses, after intravenous injection of nonionic contrast medium iohexol (Omnipaque; 300 mgI/mL, 1–1.2 mL/kg), with images acquired in the venous phase (60 seconds). Precontrast unenhanced scans are not routinely acquired to reduce radiation exposure. The scans were acquired using Siemens SOMATOM Definition edge 64-slice multidetector CT machine (Erlangen, Germany) and 1.5-mm-thin reconstructions were used for reporting and evaluation, while 5-mm axial slices were usually used for printing films.

Image Analysis

The radiological features were interpreted by two radiologists (E.D. and C.S.H.), and any doubt or discordance was addressed with mutual consensus. Quantitative parameters like size, mean postcontrast attenuation, and qualitative parameters including location, margins, enhancement, internal characteristics, infiltration of the chest wall or mediastinum, and background lung changes were recorded as follows:

- **Size:** The longest dimension in any plane was recorded.
- **Location:** In terms of the lung and lobe; central or peripheral location.
- **Margins**[15,16]: Circumscribed (well-demarcated outline for more than 75% of the mass), lobulated (smooth undulations/bulges due to uneven growth rate), and spiculated (radial extensions from margins due to

interlobular septal thickening or fibrosis by obstruction of pulmonary vessels/lymphatics).

- **Enhancement:** Homogeneous (uniform enhancement) or heterogeneous (variable enhancement).
- **Attenuation:** The mean postcontrast attenuation of the enhancing areas of the mass and that of the adjacent muscle (trapezius, latissimus dorsi, or pectoralis major) were noted. Care was taken to avoid inclusion of necrotic areas or blood vessels or fat densities within the region of interest (ROI) in both measurements.
- **Internal characteristics:** Presence or absence of fat/calcification/cavitation (presence of air or air–fluid level within)/necrosis (differential attenuation or fluid within the mass).
- **Infiltration of chest wall**[17]: Visible mass extending into the chest wall with or without rib destruction or loss of extrapleural fat.
- **Mediastinal invasion**[18]: Tumor contact with mediastinum >3 cm/more than 90-degree circumferential contact with vessels/absent mediastinal fat plane/compression of mediastinal structure/contiguous mediastinal pleural or pericardial thickening.
- **Background lung changes** were recorded for presence of chronic obstructive pulmonary disease (emphysema with or without fibrosis).
- **Lymph nodal metastasis:** Lymph node assessment included regional and nonregional nodes. Regional nodes studied as per the International Association for the Study of Lung Cancer (IASLC) nodal map included (1) supraclavicular zone, station 1 (low cervical below the lower margin of cricoid cartilage, supraclavicular and sternal notch); (2) Upper zone, stations 2 to 4 (superior mediastinal nodes including right and left upper paratracheal, prevascular, retrotracheal, right and left lower paratracheal nodes); (3) aortopulmonary zone, stations 5 and 6 (sub aortic and para-aortic nodes); (4) subcarinal zone, station 7 (subcarinal nodes); (5) lower zone, stations 8 and 9 (paraesophageal and pulmonary ligament nodes); (6) hilar zone, stations 10 and 11 (hilar and interlobar nodes); and (7) peripheral zone, stations 12 to 14 (lobar, segmental, and subsegmental nodes). The presence of nonregional lymph nodes (other cervical, abdominal, or retroperitoneal nodes) was considered as distant metastasis. Lymph nodes sizes of more than 10 mm in short axis diameter (>13 mm in subcarinal region) with or without heterogeneous enhancement and round shape was considered suspicious for nodal metastasis.
- **Distant metastasis:** Screening of the abdomen and the brain was also routinely done for all newly diagnosed lung masses as per the institute's protocol. Hence, the presence of metastases to the intra-abdominal organs, brain, and bone was assessed in addition to nodal metastasis.
- Details of **response assessment and occurrence of new metastases** were obtained from the available follow-up imaging and recorded.

Statistical Analysis

The data were transformed into variables, coded, entered in Microsoft Excel, and analyzed using SPSS software version 28. Quantitative data were expressed in mean and ranges and qualitative data were expressed in percentage. Statistical significance ($p < 0.05$) was calculated using *t*-test or analysis of variance (ANOVA) for mean and chi-squared test or Fisher's exact test for categorical variables.

Results

A total of 193 patients with lung masses who underwent CECT of the thorax were identified, out of which 68 patients could be included for the study and 125 who did not fulfil the inclusion criteria were excluded (►**Fig. 1**). Primary pulmonary sarcoma was seen in 12 patients including SS in 5 patients and Ewing's sarcoma, liposarcoma, desmoplastic round cell tumor (DSRCT), undifferentiated sarcoma (UDS), *SMARCA4*-deficient undifferentiated tumor, inflammatory myofibroblastic tumor (IMFT), and sarcomatoid carcinoma in 1 patient each (►**Figs. 2-11**) The mean age for PLS was 40.75 ± 16.17 years (mean ± SD), while the mean age for PLC was 54.8 ± 11.71 years, with a significant difference ($p = 0.001$). While carcinoma (male:female = 4.1:1) was more common in men, sarcoma showed no gender predilection ($p = 0.028$). Among carcinomas, adenocarcinoma was the most common (50%), followed by squamous cell carcinoma (28.5%), small cell carcinoma (10.7%), non-small-cell carcinoma, not otherwise specified (10.7%). Association with smoking was seen in 8.3% of sarcoma (1/12) and 53.6% of carcinoma (30/56), which showed a statistically significant difference ($p = 0.004$). ►**Table 1** summarizes the imaging characteristics of various sarcomatous tumors in our study.

Site and Size

Seven PLS were entirely pulmonary, two were pleuropulmonary, two extrapleural with extension into the lung, and one filled the entire right hemithorax. Involvement of the parahilar (75%, $p = 0.021$) and hilar regions (41.7%, $p = 0.006$) was more commonly seen in sarcomas, likely due to their large size. They were significantly more common in the lower lobes (75%, $p = 0.002$), but showed no side preference. Carcinomas were slightly more common in the right lung (58.9%, $p = 0.570$) and in the upper lobe (64.2%, $p = 0.060$), without significant difference. Peripheral (58.9%, $p = 0.570$) regions, followed by parahilar (33.9%) and hilar (7.1%) regions, were seen with carcinoma. The average size (13.19 ± 5.5 cm) was significantly higher ($p = 0.001$) in PLS patients than in PLC patients (5.68 ± 2.9 cm).

Primary Lesion

Most carcinomas were irregular in shape (83.9%, $p = 0.010$) and had spiculated margins (73.2%, $p < 0.001$). One-fourth had lobulated margins and only one of the masses was circumscribed. Oval shape was significantly more common in sarcomas (41.6%, $p = 0.003$), with either lobulated (75%, $p = 0.002$) or circumscribed margins (25%, $p = 0.015$). Calcification was also more common in sarcomas, seen in half of the masses ($p = 0.010$). None of the sarcomas showed cavitation except for the sarcomatoid carcinoma, while up to 23.2% lung carcinomas showed cavitation, although the

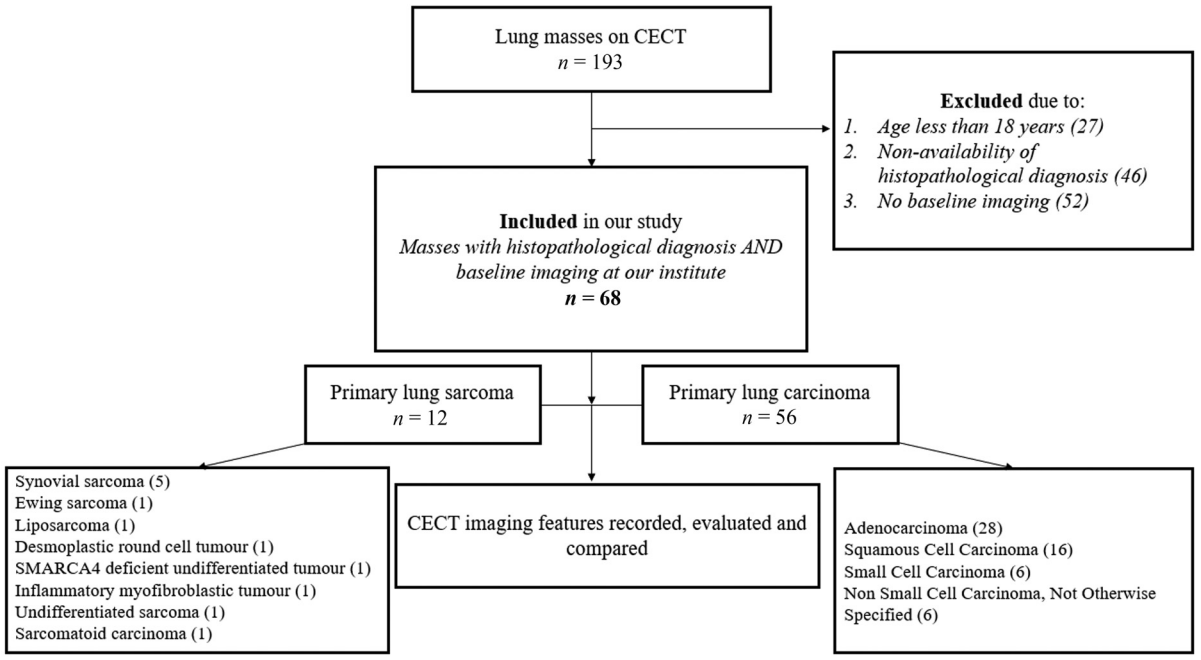

Fig. 1 Flowchart demonstrating the study protocol. CECT, contrast-enhanced computed tomography.

difference was not statistically significant ($p = 0.435$). Necrosis was commonly seen in both PLS and PLC ($p = 0.156$). The distribution of significant features between PLS and PLC is shown in ►**Table 2**.

Postcontrast Attenuation

The mean postcontrast attenuation of sarcoma was 57.3 HU and was always less than the adjacent muscle (mean: 59.4 HU), except for IMFT (mean: 145 HU). Liposarcoma showed the least attenuation of 21 HU. The mean attenuation of carcinoma was higher at 77.3 HU and 83.6% of the lesions showed a mean attenuation higher than the adjacent muscle (mean: 59.4 HU). This difference in mean postcontrast attenuation between sarcomas and carcinomas was statistically significant ($p = 0.001$)

Local Extension

Sarcomas showed transfissural extension, mediastinal invasion, and vascular encasement in 6 patients (50%) each, bronchial encasement in 4, cutoff in 2, and endobronchial extension in 1 patient. Chest wall infiltration and bony erosions were only seen with Ewing's sarcoma and the *SMARCA4*–DTS. Among these features, only the presence of fissural extension showed statistically significant difference ($p = 0.010$) and it was higher in sarcomas than in carcinomas, likely due to the larger size of sarcomas at presentation. Although not statistically significant, carcinomas were often infiltrative with 50% patients showing mediastinal invasion ($p = 1$), bronchial involvement including bronchial cutoff in 23.2% patients ($p = 1$), bronchial encasement in 26.8% patients ($p = 0.727$), chest wall infiltration in 30.4% patients ($p = 0.487$), vascular encasement 37.5% patients ($p = 0.422$), and rib or vertebral erosions in 16.1% patients ($p = 1$).

Background Changes

Emphysema was seen in one case of sarcoma (8.3%) and 32.1% carcinomas ($p = 0.156$), without significant difference.

Lymph Node Metastasis

Nodal metastasis was seen in 55.4% of carcinomas, including 25% in the ipsilateral nodes, 16.1% in the contralateral regional nodes, and 14.3% the nonregional distant lymph nodes. Only three sarcoma patients showed nodal metastasis, all to the ipsilateral lymph nodes ($p = 0.109$).

Lung, Pleural, and Distant Metastasis

About 58.9% of the carcinomas showed metastasis to the lung, pleura, brain, or abdominal viscera. In contrast, only one case of PLS showed lung metastasis and no other distant organ metastasis was seen ($p = 0.002$). Lymphangitis carcinomatosa was seen only in carcinomas (7.1%, $p = 1$).

Follow-Up Imaging

The median duration of follow-up imaging in both groups together was 11 months (range: 1–50 months). Complete response was seen in three sarcoma patients postsurgery. Unresectable cases of sarcoma and carcinoma underwent chemotherapy, radiotherapy, and/or immunotherapy. None of the sarcomas showed appearance of new metastases on follow-up imaging. On the other hand, progressive disease was seen in approximately 53.8% carcinoma patients. Metastases at baseline was present in 33 carcinoma patients with

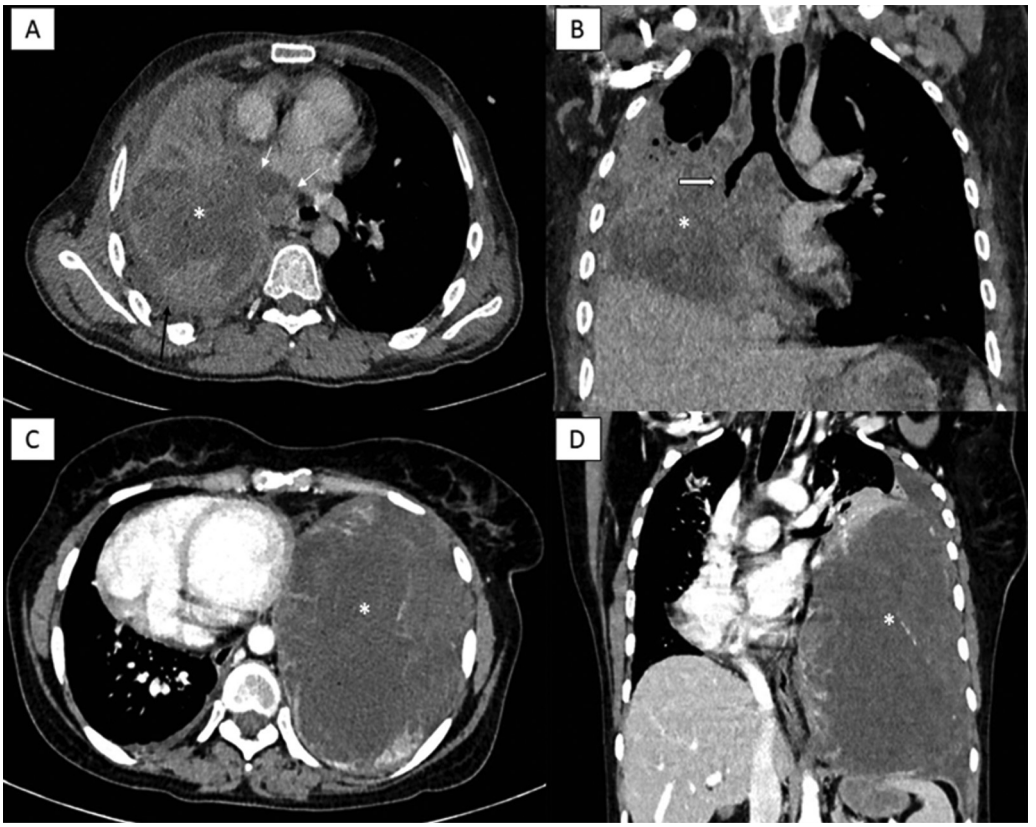

Fig. 2 Computed tomography (CT) features of synovial sarcoma. (**A**,**B**) Axial and coronal contrast-enhanced computed tomography (CECT) images of a 36-year-old man presenting with chest pain and dyspnoea show a heterogeneous parahilar mass (*asterisk*) extending into the right lower lobe with fissural extension, mediastinal invasion (*white arrows*), and bronchial narrowing (*thick arrow*) and minimal right pleural effusion (*black arrow*). (**C**) Axial and (**D**) coronal CECT images of a 28-year-old woman presenting with cough and dyspnoea show a large circumscribed pleuropulmonary mass in the left hemithorax (*asterisk*) with necrosis and collapse of the lung parenchyma. Both lesions were proven to be synovial sarcoma by biopsy.

18 more patients developing metastases on follow-up imaging ($p = 0.027$).

Differences in Imaging Features among Various Types of Carcinomas

Significant difference was seen between the four types of carcinomas in terms of mean age of presentation ($p = 0.028$), mean maximum size of the lesion ($p = 0.014$), association with smoking ($p = 0.033$), and the presence of vascular infiltration ($p = 0.022$). The mean age of presentation was highest for squamous cell carcinoma (60.81 ± 9.68 years) and least for small cell carcinoma (50.67 ± 11.84 years). The mean maximum size was highest with non-small-cell carcinomas NOS (8.1 cm), and least with adenocarcinomas (4.6 cm). The highest association with smoking was seen with small cell carcinomas (83.3%) and squamous cell carcinomas (75%). Vascular infiltration was highest with small cell carcinomas (83.3%).

Although the rest of the imaging features did not show a statistically significant difference ($p > 0.05$), adenocarcinoma was comparatively more common in females with a male-to-female ratio of 3.5:1, was peripherally located (64.3%), and had the maximum proportion of distant metastases (67.9%) including the opposite lung, pleura, adrenal gland, brain, bone, liver, kidney, spleen, and omentum. Lymphangitis carcinomatosa was also seen only with adenocarcinoma (14.3%). Squamous cell carcinoma was more common in men (male:female ratio 15:1), showed highest incidence of chest wall extension (50%), and high incidence of cavitation (31.3%), calcification (25%), necrosis (68.8%), and background emphysema (50%). All the six cases of small cell carcinoma were seen in men, and they showed the highest mean postcontrast attenuation (80.67 HU), highest incidence of mediastinal invasion (83.3%), and lymph nodal metastasis (83.3%). Non-small-cell carcinoma, NOS was predominantly peripheral (83.3%), large in size, with cavitation (33.3%), necrosis (50%), and lymph nodal metastasis (50%).

Discussion

A vast majority of lung malignancies are carcinoma and approximately 80 to 87% carcinomas are of the non-small-cell type.[19] As per the 2021 WHO classification, malignant lung neoplasms include adenocarcinoma, squamous cell carcinoma, neuroendocrine carcinomas (small cell and large cell carcinoma), carcinoid, and other less common entities in the lung such as mesenchymal tumors, Perivascular Epithelioid Cell neoplasms (PEComas), hematolymphoid tumors,

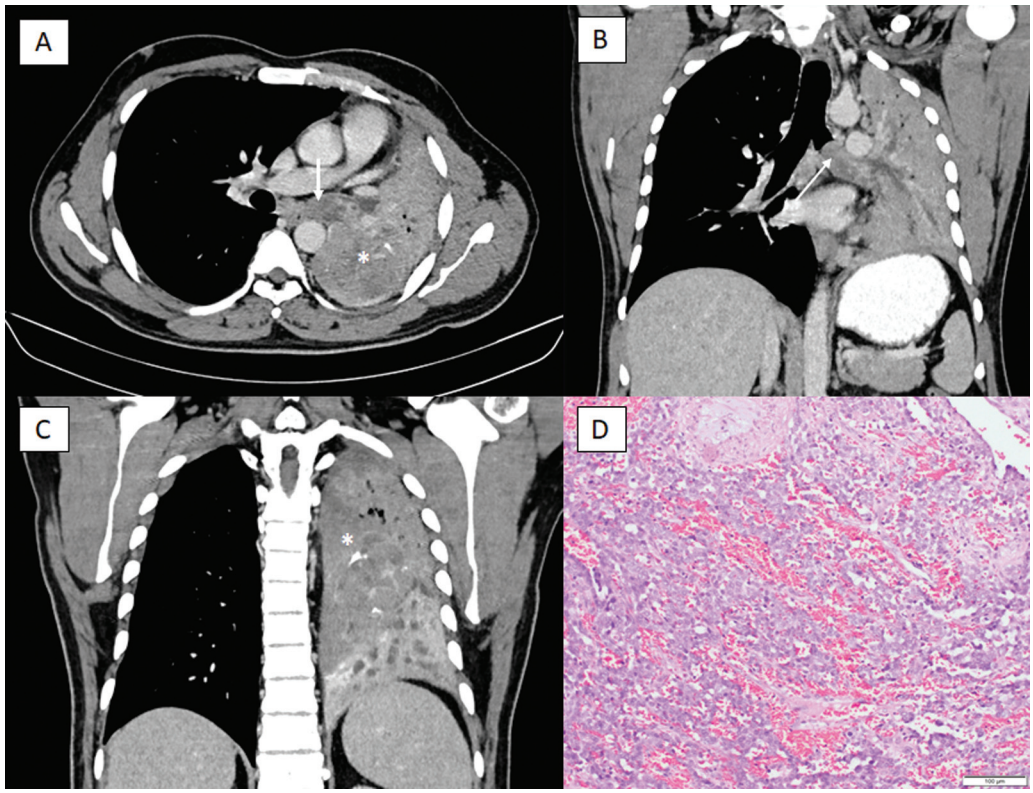

Fig. 3 Endobronchial extension of synovial sarcoma. (**A**) Axial and (**B,C**) coronal reformatted contrast-enhanced computed tomography (CECT) images of a 38-year-old man, a farmer, presenting with cough, expectoration, and dyspnoea show a mass in the left lower lobe (*asterisk*) with extension into the lobar bronchus (*arrow*) and resultant lung collapse. (**D**) Hematoxylin and eosin (×100) staining of biopsy core showed multiple spindle cells showing round hyperchromatic nuclei and occasional glandular components. Further evaluation for SSX translocation was positive on in situ hybridization.

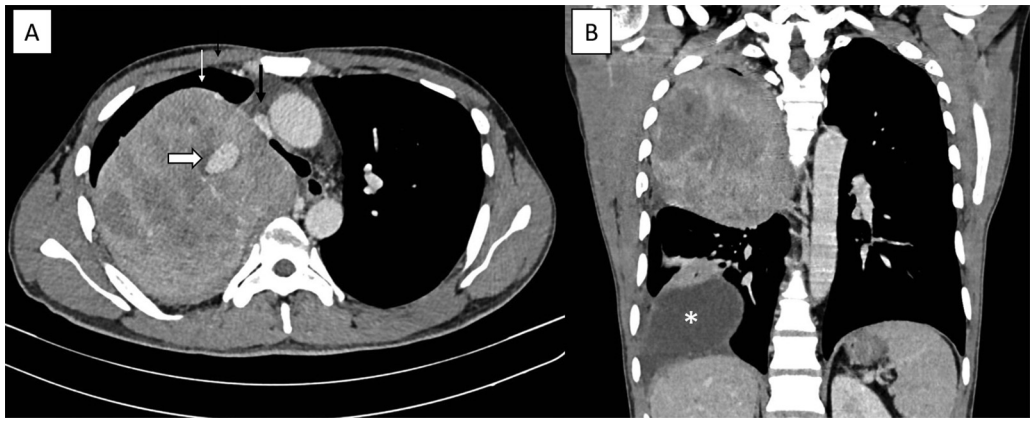

Fig. 4 Computed tomography (CT) features of synovial sarcoma. (**A**) Axial and (**B**) coronal reformatted contrast-enhanced computed tomography (CECT) images of a 25-year-old man with chest pain and hemoptysis show a right upper lobe mass with an intratumoral pseudoaneurysm (*thick arrow*), partial superior vena cava (SVC) compression (*black arrow*), circumscribed margins despite the large size (*white arrow*), and loculated pleural effusion (*asterisk* in **B**), proven to be synovial sarcoma by biopsy.

and tumors of ectopic tissue.[9] Adenocarcinoma is the most common subtype in women and nonsmokers, and is usually a peripherally located nodule or mass, can show surrounding ground glass opacities, and metastasis to liver, bone, brain, adrenals, and lung. Squamous cell carcinoma is usually seen in smokers as a centrally located mass with cavitation, and may be associated with segmental or lobar collapse and Pancoast's syndrome. Small cell carcinoma is also associated with smoking and is seen as a centrally located mass with the superior vena cava (SVC) infiltration or obstruction and bulky mediastinal lymph nodal metastases, mimicking lymphoma.[19] Large cell carcinoma (on histopathology examination postresection),

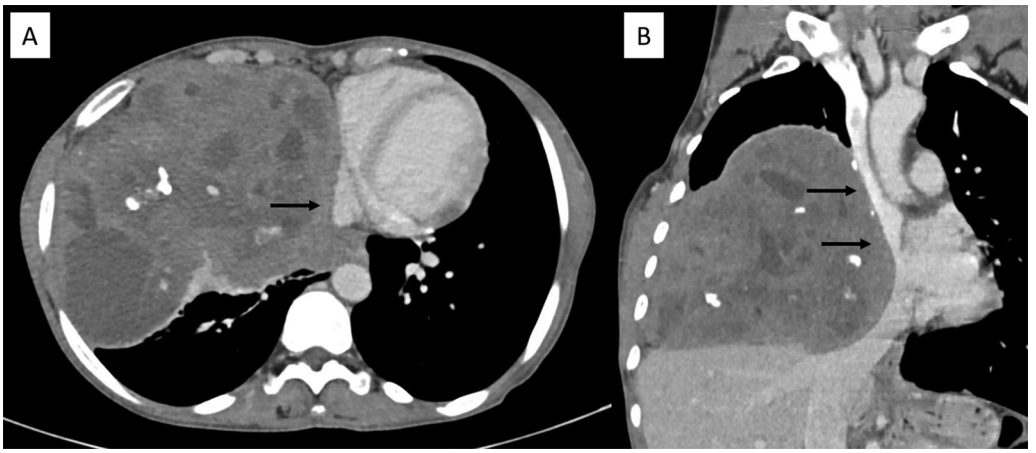

Fig. 5 Desmoplastic small round cell tumor (DSRCT) of pleural origin in a 46-year-old woman with dyspnoea and facial puffiness. (**A**) Axial and (**B**) coronal reformatted contrast-enhanced computed tomography (CECT) shows a heterogeneously enhancing mass with necrosis and calcifications compressing the superior vena cava (SVC) and right atrium (*black arrows*).

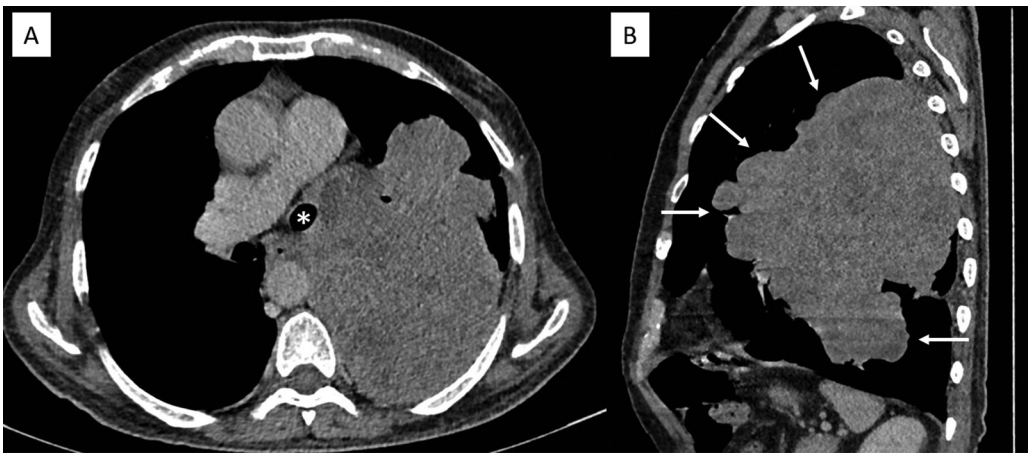

Fig. 6 Undifferentiated sarcoma in a 60-year-old man presenting with dyspnea, cough with expectoration. (**A**) Axial and (**B**) sagittal reformatted contrast-enhanced computed tomography (CECT) images show lobulated margins (*white arrows*) of the mass in the left lower lobe and bronchial encasement (*asterisk*).

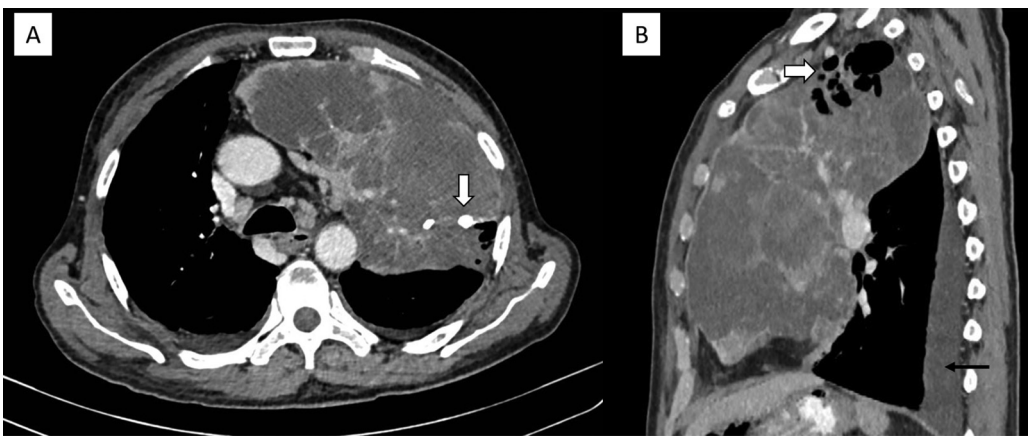

Fig. 7 Sarcomatoid carcinoma in a 68-year-old man, smoker, presenting with dyspnea, cough, and chest pain. (**A**) Axial and (**B**) sagittal reformatted contrast-enhanced computed tomography (CECT) images show a large necrotic mass involving the entire left upper lobe with the presence of calcifications (*arrow* in **A**), cavitation (*arrow* in **B**), and mild left pleural effusion (*black arrow* in **B**).

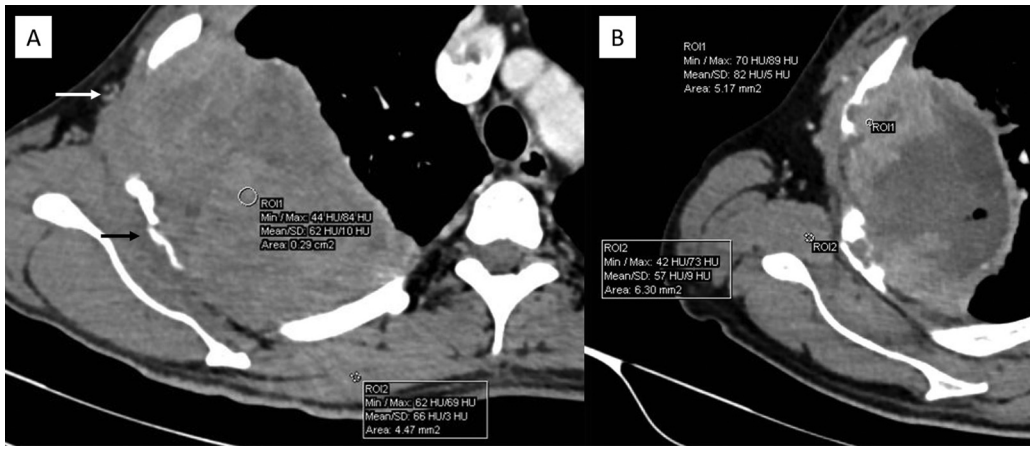

Fig. 8 Difference in postcontrast attenuation of lung masses. (**A**) Axial contrast-enhanced computed tomography (CECT) image shows an irregular lobulated mass with areas of necrosis, chest wall infiltration (*white arrow* in **A**) and rib destruction (*black arrow* in **A**). The postcontrast attenuation of the mass (62 HU) is less than the adjacent muscle (66 HU). This was proven to be *SMARCA4*-deficient undifferentiated tumor on biopsy. (**B**) In comparison, attenuation of the squamous cell carcinoma was 82 HU in a different patient where muscle showed an attenuation of 57 HU.

Fig. 9 Ewing's sarcoma in an 18-year-old woman presenting with chest pain. (**A**) Axial and (**B**) sagittal reformatted contrast-enhanced computed tomography (CECT) images show a heterogeneous mass with necrosis, chunky calcifications, and adjacent rib sclerosis and erosion (*thick arrow*).

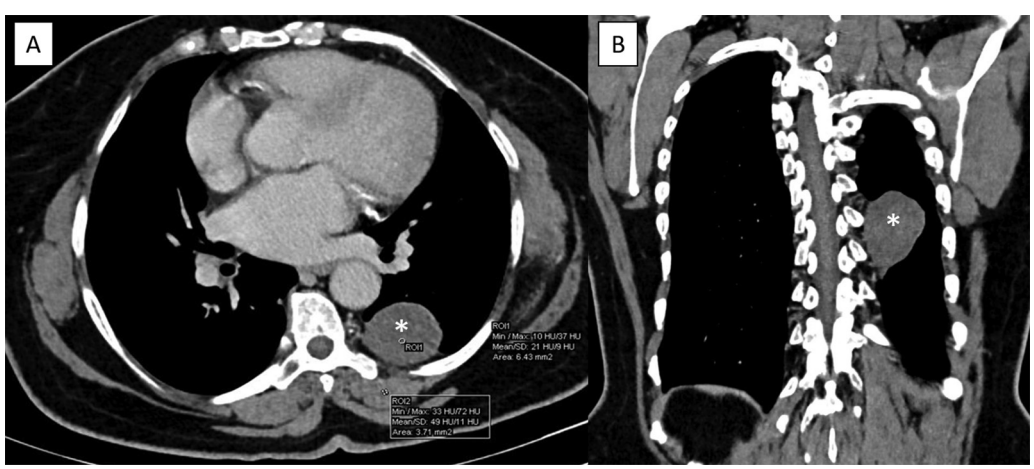

Fig. 10 Liposarcoma in a 54-year-old woman presenting with back pain and incidentally detected mass on radiograph. (**A**) Axial and (**B**) coronal reformatted contrast-enhanced computed tomography (CECT) images show a circumscribed mass of extrapleural origin (*asterisk*) with a mean of 21 HU, proven to be round cell liposarcoma by biopsy.

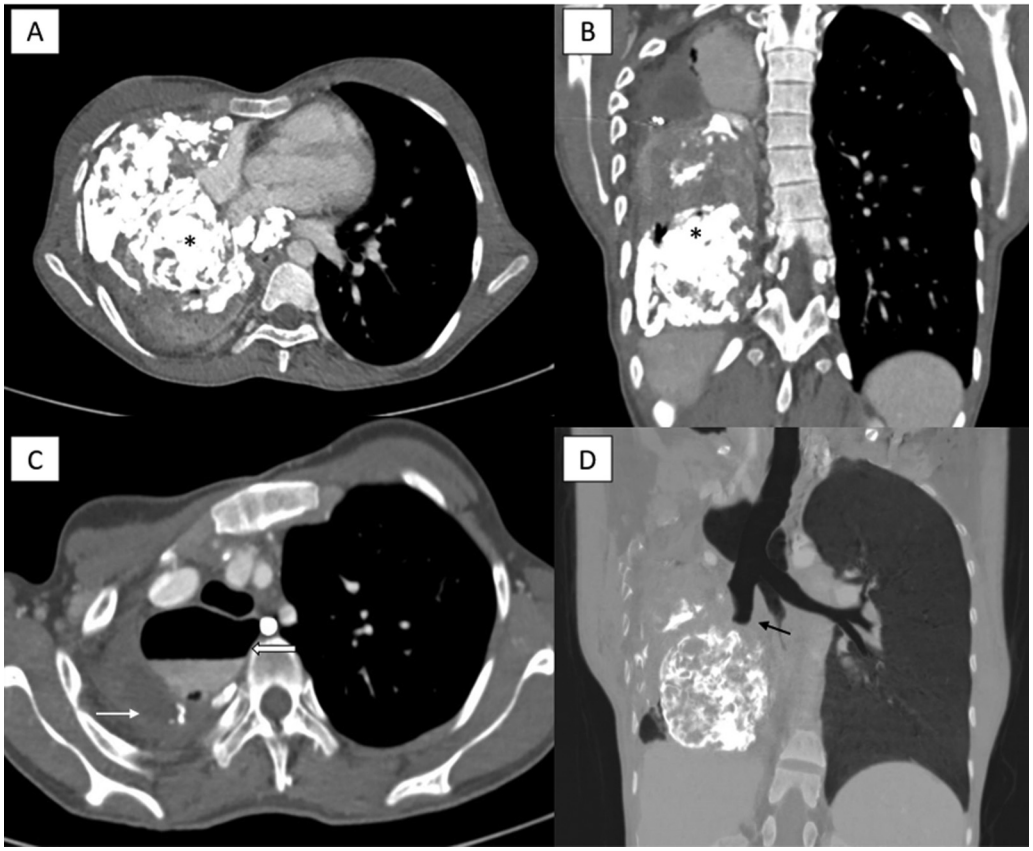

Fig. 11 Inflammatory myofibroblastic tumor (IMFT) in a 23-year-old woman presenting with cough, hemoptysis, dyspnea, and dysphagia. Mediastinal and lung windows of axial (**A**,**C**) and coronal reformatted (**B**,**D**) contrast-enhanced computed tomography (CECT) images show a large mass with chunky calcification (*asterisk*) occupying almost the entire right lung, with cutoff of the right main bronchus (*black arrow* in **D**), mediastinal extension, and rib crowding in the right upper lobe with loculated pleural effusion (*white arrow* in **C**). Note the deviated dilated esophagus with air fluid level (*thick arrow* in **C**).

also referred to as non-small-cell carcinoma, NOS (on examination of biopsy/cytology specimen) is centrally located, large in size, with bulky lymph nodal metastasis.[9,19] CECT enables identification of the primary malignancy, estimation of its extent, evaluation of distant metastasis, and staging and prognostication. The final diagnosis of lung malignancies is through histopathology, immunohistochemistry, and molecular techniques.

Sarcomas of the lung account for 9% among all soft-tissue sarcomas and less than 1% of primary lung malignancies.[20] As per the 2020 WHO classification of soft-tissue tumors, they are included under malignant tumors of uncertain differentiation and are considered to be arise from undifferentiated mesenchymal stem cells.[14,21] The most common type of malignancy among sarcomas in our study was SS (►**Figs. 2**–**14**). Various authors have documented occurrence of SS in the 25- to 39-year age group, with no gender or side predilection.[22] The lesions can be completely intrapulmonary or pleuropulmonary, rarely endobronchial, and the size ranges between 7 and 10 cm, larger than carcinoma.[23–25] This larger size at presentation could be attributed to the late occurrence of bronchovascular infiltration and, hence, late onset of symptoms.[22,26] Most masses in SS show circumscribed or lobulated margins, heterogeneous contrast enhancement, and areas of necrosis.[22,26] The imaging features of SS in our study correlated well with previous studies (►**Table 3**). In addition, in our study, we observed that the average attenuation of SS was 51.4 HU (57.3 HU for all sarcomas), was much less than carcinoma (77.3 HU), and always less than that of the adjacent muscle. Bronchial involvement can include narrowing and endobronchial extension (►**Fig. 3**), but complete bronchial cutoff has not been described in SS, unlike carcinoma. Histopathological diagnosis of SS needs detection of Synovial Sarcoma, X (SSX) mutation by Polymerase Chain Reaction (PCR) or Fluorescent In Situ Hybridization (FISH), which can be found in up to 95% cases.[27,28] This mutation is caused by translocation between chromosomes X and 18, t(X;18) (p11.2; q11.2), creating SYT–SSX fusion protein, which interferes with chromatin remodeling.

Among other sarcomas included in our study, Ewing's sarcoma usually originates from the chest wall and pulmonary parenchymal disease may be seen in 25% cases.[29] Previously considered as a sarcoma, sarcomatoid carcinoma is now a subtype of non-small-cell carcinoma. They are a group of poorly differentiated carcinomas with sarcoma components or sarcomalike differentiation in histology.[30] They also present in old age with a male predilection, in smokers, and have poor prognosis.[31] In our study, we included the sarcomatoid carcinoma (►**Fig. 7**) under the sarcoma

Table 1 Imaging characteristics of various intrathoracic sarcomatous tumors in our study

Sl. no.	Age (y)	Sex	Site	Size (cm)	HU	Shape	Margins	Cavitation	Calcification	Necrosis	Fissural extension	Mediastinal invasion	Vascular encasement	Bronchial cutoff/ narrowing	Chest wall infiltration	Background emphysema	Metastasis	Final HPE
1	36	M	RLL, parahilar	9.6	38	Irregular	Lobulated	−	−	+	+	+	+	+	−	−	+ (nodal)	Synovial sarcoma
2	38	M	RLL + endobronchial, hilar, and parahilar	8.9	56	Round	Lobulated	−	+	+	−	+	−	−	−	−	−	Synovial sarcoma
3	28	F	Left pleuropulmonary	19.3	44	Oval	Circumscribed	−	−	+	−	−	−	−	−	−	−	Synovial sarcoma
4	57	F	RLL, parahilar	7.5	51	Oval	Lobulated	−	+	+	+	−	+	−	−	−	−	Synovial sarcoma
5	25	M	RUL, parahilar	13.7	68	Oval	Circumscribed	−	−	+	_	+	+	+	−	−	−	Synovial sarcoma
6	68	M	LUL, parahilar	22.5	35	Irregular	Lobulated	+	+	+	_	_	+	+	−	+	+ (nodal)	Sarcomatoid carcinoma
7	60	M	LLL, hilar, and parahilar	19.5	40	Oval	Lobulated	−	−	+	+	+	+	+	−	−	+ (lung)	Undifferentiated sarcoma
8	36	M	RUL, peripheral	15.4	62	Irregular	Lobulated	−	−	+	+	−	−	−	+	−	−	*SMARCA4*-deficient undifferentiated tumor
9	46	F	Right pleuropulmonary	16.2	60	Irregular	Lobulated	−	+	+	−	+	−	+	−	−	−	Desmoplastic small round cell tumor
10	18	F	Left extrapleural with pulmonary extension	7.7	68	Irregular	Lobulated	−	+	+	+	−	−	−	+	−	−	Ewing's sarcoma
11	54	F	LLL + extrapleural	5.1	21	Oval	Circumscribed	−	−	−	−	−	−	−	−	−	−	Round cell liposarcoma
12	23	F	Entire right hemithorax	12.9	145	Irregular	Lobulated	−	+	+	+	+	+	+	−	−	+ (nodal)	Inflammatory myofibroblastic tumor

Abbreviations: HPE, Histo Pathological Examination; LLL, left lower lobe; LUL, left upper lobe; RLL, right lower lobe; RUL, right upper lobe.

Table 2 Comparison of significant differences between PLC and PLS

Parameter	Carcinoma *n*, %	Sarcoma *n*, %	*p*-Value
Features more common in lung sarcoma			
Age <40 y	4 (7.1)	7 (58.3)	<0.001
Female sex	11 (19.6)	6 (50)	0.028
Nonsmoker	26 (46.4)	11 (91.7)	0.004
Size >6 cm	19 (33.9)	11 (91.7)	<0.001
Postcontrast attenuation <60 HU	9 (16.1)	7 (58.3)	0.001
Lower lobe involvement	18 (32.1)	9 (75)	0.002
Parahilar location	19 (33.9)	9 (75)	0.021
Hilar location	4 (7.1)	5 (41.7)	0.006
Oval shape	5 (8.9)	5 (41.7)	0.003
Circumscribed margin	1 (1.8)	3 (25)	0.015
Lobulated margin	14 (25)	9 (75)	0.002
Presence of calcification	9 (16.1)	6 (50)	0.010
Fissural extension	9 (16.1)	6 (50)	0.010
Absence of organ metastasis	23 (41.1)	11 (91.7)	0.002
Features more common in lung carcinoma			
Age >40 y	52 (92.9)	5 (41.7)	<0.001
Male sex	45 (80.4)	6 (50)	0.028
Smoker	30 (53.6)	1 (8.3)	0.004
Size <6 cm	37 (66.1)	1 (8.3)	<0.001
Postcontrast attenuation >60 HU	47 (83.9)	5 (41.7)	0.001
Irregular shape	47 (83.9)	6 (50)	0.010
Spiculated margin	41 (73.2)	0 (0)	<0.001
Absence of calcification	47 (83.9)	6 (50)	0.010
Absence of fissural extension	47 (83.9)	6 (50)	0.010
Presence of organ metastasis	33 (58.9)	1 (8.3)	0.002
New metastasis on subsequent imaging	18 (32.1)	0 (0)	0.027

Abbreviations: PLS, primary lung sarcoma; PLC, primary lung carcinoma.

group due to overlapping imaging features such as large size, low attenuation of 35 HU, presence of necrosis, and calcification, causing bronchial cutoff and associated background emphysema. Other sarcomas included in our study, namely, liposarcoma, IMFT, *SMACA4*–DTS, and DSRCT, are rare in the thorax, with only a handful of cases with imaging features reported in literature.[32–35]

In contrast to sarcoma, lung carcinomas have a smaller mean size (< 4 cm in adenocarcinomas) and the imaging characteristics depend on their pathological type. They can be seen in the peripheral lung or parahilar/hilar region with or without bronchial cutoff, presence of cavitation (particularly squamous cell carcinoma), and spiculated margins, and surrounding satellite nodules are seen in most carcinomas[36] (►**Figs. 12**—**14**). They often show contiguous extension with mediastinal lymph nodes and have a propensity for distant visceral metastases.[37] As per previous studies, approximately 5.5% of PLCs are associated with lymphangitis carcinomatosa, a feature not described in PLS.[38] In our study, carcinoma frequently showed a higher mean age, male predilection, smaller size at presentation, higher mean postcontrast attenuation, irregular shape, spiculated margins, and frequent distant metastasis with statistically significant difference. Background emphysematous changes, although not statistically significant, were seen 32.1% of carcinomas and only in one patient with sarcomatoid carcinoma, likely due to the higher association with smoking in carcinomas. Features like necrosis, mediastinal invasion, and vascular encasement were seen in both carcinoma and sarcoma.

Multimodality therapies of lung carcinoma and sarcoma includes surgical resection, chemotherapy, and radiotherapy. However, due to the rarity of lung sarcoma, there is no

Table 3 Imaging characteristics of synovial sarcoma of the lung in previous studies

Sl. no.	Case studies/reports	Mean/ median age (y)	Sex (M: F)	Most common site	Mean maximum size (cm)	Contour (most common)	Internal characteristics	Local extension	Background lung/thorax	Metastasis/ recurrence
1	Hartel et al[26] ($n=34$): 34/58 lung, rest pleural and mediastinal	42	1.1:1	Lung (among lung, pleura and mediastinum)	7.5	Circumscribed	Homogeneous or heterogeneous enhancement, necrosis. No calcification/ cavitation	No bone destruction or chest wall infiltration/ lymph nodes	Ipsilateral pleural effusion	Recurrence in 7 cases, metastasis in 8 cases
2	Frazier et al[22] ($n=11$): pleuropulmonary	37	1: 1.4	Right lung, peripheral or para fissural	10	Round/ovoid/ lobulated	Heterogeneous with necrosis	No chest wall infiltration or bone destruction	Pleural effusion (7/11)	Pleural metastasis (2/11)
3	Essary et al[23] ($n=9$)	31	1.4: 1	Left lung	7.2	Circumscribed	Heterogeneous with necrosis	One of them showed endobronchial extension	–	Distant metastasis (3/11), local recurrence (8/11)
4	Kim et al[41] ($n=6$): 14 thoracic	37	1: 1.3	Lung (among thoracic tumors)	10.2	Circumscribed	Necrosis, enhancing solid areas, and intratumoral vessels	Extrapleural or chest wall extension, but no bony erosions	Pleural effusion (7/14)	Lung metastasis
5	Zhang et al[42] ($n=5$)	49	4: 1	Right lung	13.2	Circumscribed	Heterogeneous enhancement, necrosis, and cystic areas	–	Pleural effusion (4/5)	Recurrence (2/5), bone metastasis (1/5)
6	Baheti et al[43] ($n=7$): 7/42 lung, rest pleural and mediastinal	45	1: 1.6	Pleura (among lung, pleura, and mediastinum)	9.1	Circumscribed	Calcifications, hemorrhage, fluid–fluid levels, bowl of grapes appearance, and triple sign	–	Pleural effusion (10/42)	Recurrence/ metastasis (28/42), local recurrence (11/ 42)
7	Synovial sarcoma in our study ($n=5$)	36.8	3: 2	Right lower lobe	11.8	Lobulated	Heterogeneous enhancement, necrosis (5/5), calcification (2/5)	Fissural (2/5) and mediastinal extension (3/5), bronchial encasement (2/5), endobronchial extension (1/5)	Pleural effusion (3/5)	Ipsilateral nodal metastasis (1/5)

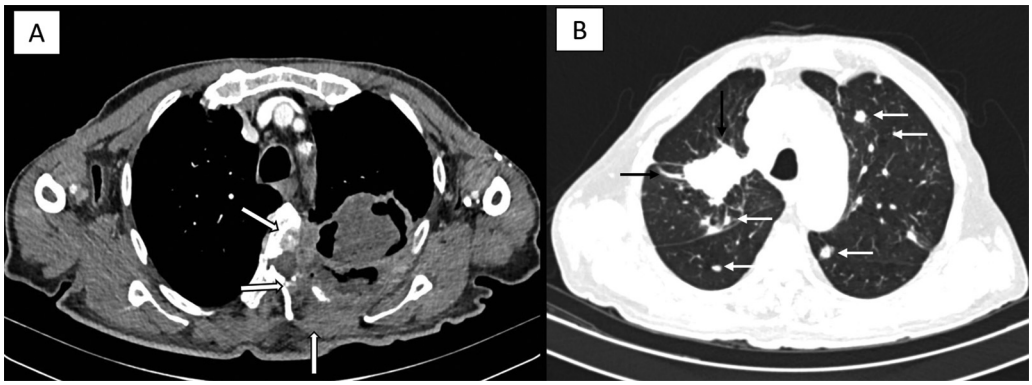

Fig. 12 Contrast-enhanced computed tomography (CECT) features of lung carcinomas. (**A**) Axial CECT image of a 71-year-old male, smoker, presenting with dyspnoea and chest pain shows a heterogeneously enhancing mass with internal cavitation and extensive infiltration into chest wall, rib, and vertebral destruction (*thick arrows*). The final histology was squamous cell carcinoma. (**B**) Lung window of axial CECT image of a 53-year-old man presenting with cough and expectoration shows a mass with spiculated margins (*black arrows*), multiple satellite nodules, nodules in adjacent lobe, and metastases in the opposite lung (*white arrows*). The final histology was poorly differentiated adenocarcinoma.

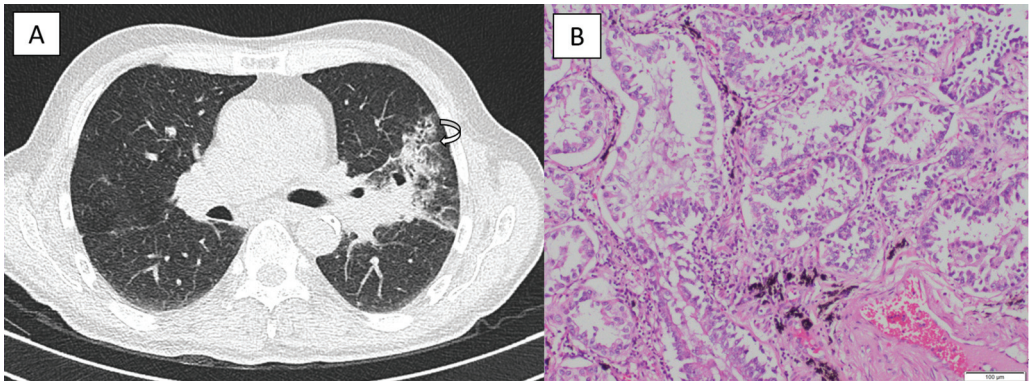

Fig. 13 Contrast-enhanced computed tomography (CECT) features of lung carcinomas. (**A**) Lung window of axial CECT image of a 56-year-old male, smoker, presenting with cough and expectoration shows an irregular mass with surrounding ground glass opacities and lymphatic spread in the form of perilymphatic nodules and septal thickening (*curved arrow*) in the left lung. (**B**) Corresponding hematoxylin and eosin (H&E; ×100) staining of biopsy specimen shows multiple glandular areas of neoplastic cells, proven to be acinic predominant adenocarcinoma.

standardized therapy regimen. Nonanatomical resection is preferred in sarcoma, compared with the anatomical resection, which is used in carcinomas.[39] Specific chemotherapeutic agents including ifosfamide and doxorubicin are used for SS, with a response rate between 24 and 50%.[11,22] Immunotherapy agents like bevacizumab and pembrolizumab have also proven useful in *SMARC4*–DTS.[40] The 5-year survival rate for lung sarcoma is better than carcinomas.[12,14]

Although the study could highlight statistically significant difference ($p < 0.05$) in mean age, size, site, shape, margins, attenuation, calcification, fissural extension, and distant metastases between sarcoma and carcinoma, it is limited by small sample size and heterogeneity within the sarcoma group due to the rarity of the disease itself. Thus, the results would need further validation with large sample size to reach definite conclusions. Since the study was retrospective, apart from smoking, association with other epidemiological factors like environmental or genetic risk factors were not explored.

Conclusion

While most of the available literatures separately depict the imaging features of an individual type of sarcoma, our study could identify similarities in the imaging features of various types of sarcoma and highlight major differences between PLS and PLC. Large size of lesion, lower lobe, parahilar or hilar location, low mean attenuation, presence of lobulated margins, calcification and fissural extension, and absence of surrounding emphysematous changes or distant metastasis in young patients are pointers to sarcoma rather than carcinoma. These imaging features can aid in establishing concordance with histopathological diagnosis of these rare malignancies and facilitate mutation testing for patients with suspicious imaging features. However, due to the small sample size and heterogeneous representation of different types of sarcomas in our study, further larger studies are needed to validate the same.

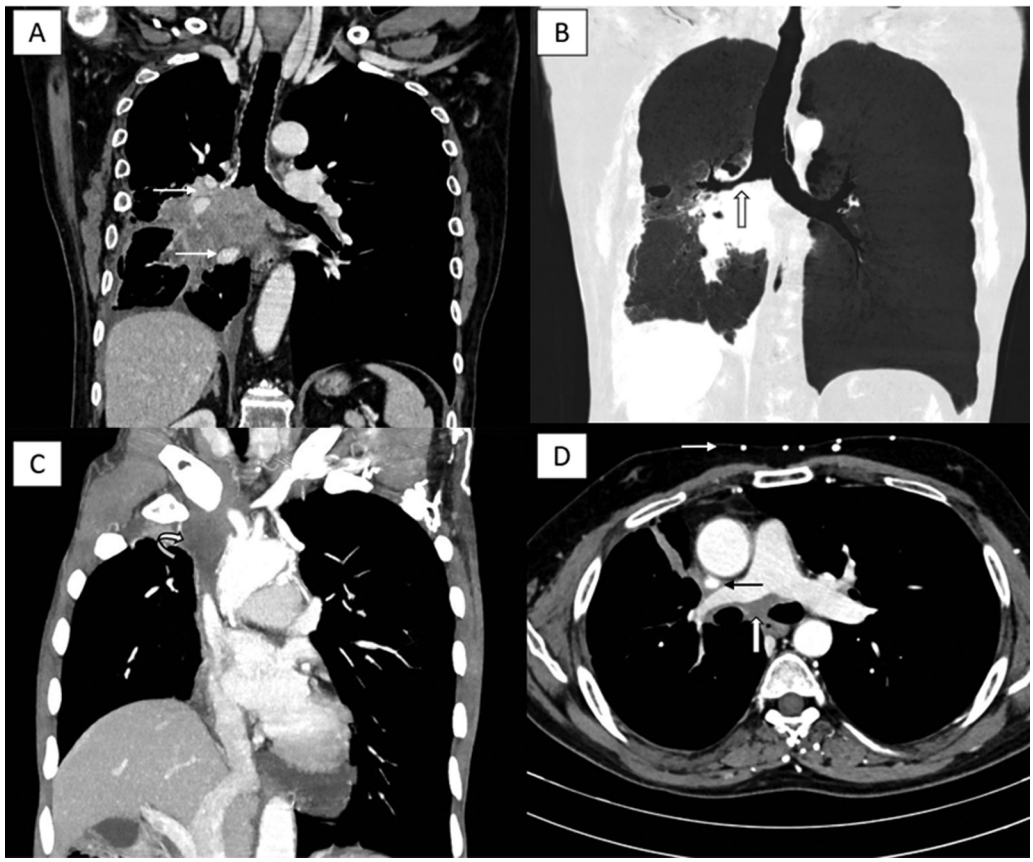

Fig. 14 Bronchovascular infiltration in lung carcinomas. Coronal (**A**) mediastinal and (**B**) lung windows of contrast-enhanced computed tomography (CECT) images in a 43-year-old male smoker shows a spiculated mass encasing the branches of the right pulmonary artery, right inferior pulmonary vein (*white arrows* in **A**) with complete cutoff of the right lower lobe bronchus and narrowing of the right main bronchus (*thick arrow* in **B**), proven to be adenocarcinoma. (**C**) Coronal CECT image of a 61-year-old man, smoker, presenting with chest pain and edema of the upper extremity shows superior vena cava (SVC) obstruction (*curved arrow*) in a poorly differentiated adenocarcinoma. (**D**) Axial CECT image of a 51-year-old man, smoker, complaining of cough and chest pain shows SVC narrowing (*black arrow*) by small cell carcinoma (*thick arrow*) with resultant formation of chest wall collaterals (*white arrow*).

Funding
None.

Conflict of Interest
None declared.

References

1 Dela Cruz CS, Tanoue LT, Matthay RA. Lung cancer: epidemiology, etiology, and prevention. Clin Chest Med 2011;32(04):605–644
2 Travis WD. Pathology of lung cancer. Clin Chest Med 2011;32(04): 669–692
3 Inamura K. Lung cancer: understanding its molecular pathology and the 2015 WHO classification. Front Oncol 2017;7:193
4 Hashimoto H, Tsugeno Y, Sugita K, Inamura K. Mesenchymal tumors of the lung: diagnostic pathology, molecular pathogenesis, and identified biomarkers. J Thorac Dis 2019;11(Suppl 1):S9–S24
5 Tomlinson J, Barsky SH, Nelson S, et al. Different patterns of angiogenesis in sarcomas and carcinomas. Clin Cancer Res 1999;5 (11):3516–3522
6 Hlatky L, Hahnfeldt P, Folkman J. Clinical application of antiangiogenic therapy: microvessel density, what it does and doesn't tell us. J Natl Cancer Inst 2002;94(12):883–893
7 Birau A, Ceausu RA, Cimpean AM, Gaje P, Raica M, Olariu T. Assessement of angiogenesis reveals blood vessel heterogeneity in lung carcinoma. Oncol Lett 2012;4(06):1183–1186
8 Gladish GW, Sabloff BM, Munden RF, Truong MT, Erasmus JJ, Chasen MH. Primary thoracic sarcomas. Radiographics 2002;22 (03):621–637
9 Nicholson AG, Tsao MS, Beasley MB, et al. The 2021 WHO classification of lung tumors: impact of advances since 2015. J Thorac Oncol 2022;17(03):362–387
10 Postmus PE, Kerr KM, Oudkerk M, et al; ESMO Guidelines Committee. Early and locally advanced non-small-cell lung cancer (NSCLC): ESMO Clinical Practice Guidelines for diagnosis, treatment and follow-up. Ann Oncol 2017;28(Suppl 4):iv1–iv21
11 Dennison S, Weppler E, Giacoppe G. Primary pulmonary synovial sarcoma: a case report and review of current diagnostic and therapeutic standards. Oncologist 2004;9(03):339–342
12 Sung H, Ferlay J, Siegel RL, et al. Global Cancer Statistics 2020: GLOBOCAN estimates of incidence and mortality worldwide for 36 cancers in 185 countries. CA Cancer J Clin 2021;71(03): 209–249
13 Régnard JF, Icard P, Guibert L, de Montpreville VT, Magdeleinat P, Levasseur P. Prognostic factors and results after surgical treatment of primary sarcomas of the lung. Ann Thorac Surg 1999;68 (01):227–231

14 Porte HL, Metois DG, Leroy X, Conti M, Gosselin B, Wurtz A. Surgical treatment of primary sarcoma of the lung. Eur J Cardiothorac Surg 2000;18(02):136–142
15 Snoeckx A, Reyntiens P, Desbuquoit D, et al. Evaluation of the solitary pulmonary nodule: size matters, but do not ignore the power of morphology. Insights Imaging 2018;9(01):73–86
16 Gurney JW. Determining the likelihood of malignancy in solitary pulmonary nodules with bayesian analysis. Part I. Theory. Radiology 1993;186(02):405–413
17 Ratto GB, Piacenza G, Frola C, et al. Chest wall involvement by lung cancer: computed tomographic detection and results of operation. Ann Thorac Surg 1991;51(02):182–188
18 Glazer HS, Kaiser LR, Anderson DJ, et al. Indeterminate mediastinal invasion in bronchogenic carcinoma: CT evaluation. Radiology 1989;173(01):37–42
19 Panunzio A, Sartori P. Lung cancer and radiological imaging. Curr Radiopharm 2020;13(03):238–242
20 Etienne-Mastroianni B, Falchero L, Chalabreysse L, et al. Primary sarcomas of the lung: a clinicopathologic study of 12 cases. Lung Cancer 2002;38(03):283–289
21 Sbaraglia M, Bellan E, Dei Tos AP. The 2020 WHO classification of soft tissue tumours: news and perspectives. Pathologica 2021; 113(02):70–84
22 Frazier AA, Franks TJ, Pugatch RD, Galvin JR. From the archives of the AFIP: pleuropulmonary synovial sarcoma. Radiographics 2006;26(03):923–940
23 Essary LR, Vargas SO, Fletcher CDM. Primary pleuropulmonary synovial sarcoma: reappraisal of a recently described anatomic subset. Cancer 2002;94(02):459–469
24 Hisaoka M, Hashimoto H, Iwamasa T, Ishikawa K, Aoki T. Primary synovial sarcoma of the lung: report of two cases confirmed by molecular detection of SYT-SSX fusion gene transcripts. Histopathology 1999;34(03):205–210
25 Leonard R, Schultz C, Hadique S. An unusual endobronchial lesion: expanding the differential diagnosis. Respirol Case Rep 2019;7 (05):e0429
26 Hartel PH, Fanburg-Smith JC, Frazier AA, et al. Primary pulmonary and mediastinal synovial sarcoma: a clinicopathologic study of 60 cases and comparison with five prior series. Mod Pathol 2007;20 (07):760–769
27 Stacchiotti S, Van Tine BA. Synovial sarcoma: current concepts and future perspectives. J Clin Oncol 2018;36(02):180–187
28 Ten Heuvel SE, Hoekstra HJ, Suurmeijer AJH. Diagnostic accuracy of FISH and RT-PCR in 50 routinely processed synovial sarcomas. Appl Immunohistochem Mol Morphol 2008;16(03):246–250
29 Takahashi D, Nagayama J, Nagatoshi Y, et al. Primary Ewing's sarcoma family tumors of the lung a case report and review of the literature. Jpn J Clin Oncol 2007;37(11):874–877
30 Weissferdt A. Pulmonary sarcomatoid carcinomas: a review. Adv Anat Pathol 2018;25(05):304–313
31 Roesel C, Terjung S, Weinreich G, et al. Sarcomatoid carcinoma of the lung: a rare histological subtype of non-small cell lung cancer with a poor prognosis even at earlier tumour stages. Interact Cardiovasc Thorac Surg 2017;24(03):407–413
32 Chen M, Yang J, Zhu L, Zhou C, Zhao H. Primary intrathoracic liposarcoma: a clinicopathologic study and prognostic analysis of 23 cases. J Cardiothorac Surg 2014;9:119
33 Panagiotopoulos N, Patrini D, Gvinianidze L, Woo WL, Borg E, Lawrence D. Inflammatory myofibroblastic tumour of the lung: a reactive lesion or a true neoplasm? J Thorac Dis 2015;7(05):908–911
34 Perret R, Chalabreysse L, Watson S, et al. SMARCA4-deficient thoracic sarcomas: clinicopathologic study of 30 cases with an emphasis on their nosology and differential diagnoses. Am J Surg Pathol 2019;43(04):455–465
35 Fois AG, Pirina P, Arcadu A, et al. Desmoplastic small round cell tumors of the pleura: a review of the clinical literature. Multidiscip Respir Med 2017;12:22
36 Hollings N, Shaw P. Diagnostic imaging of lung cancer. Eur Respir J 2002;19(04):722–742
37 Quint LE, Tummala S, Brisson LJ, et al. Distribution of distant metastases from newly diagnosed non-small cell lung cancer. Ann Thorac Surg 1996;62(01):246–250
38 Im Y, Lee H, Lee HY, et al. Prognosis of pulmonary lymphangitic carcinomatosis in patients with non-small cell lung cancer. Transl Lung Cancer Res 2021;10(11):4130–4140
39 Gołota J, Osowiecka K, Orłowski T. Primary pulmonary sarcoma: treatment outcomes depending on the different types of radical operation. Kardiochir Torakochirurgia Pol 2019;16(01):1–6
40 Takada K, Sugita S, Murase K, et al. Exceptionally rapid response to pembrolizumab in a SMARCA4-deficient thoracic sarcoma overexpressing PD-L1: a case report. Thorac Cancer 2019;10(12):2312–2315
41 Kim GH, Kim MY, Koo HJ, Song JS, Choi CM. Primary pulmonary synovial sarcoma in a tertiary referral center: clinical characteristics, CT, and 18F-FDG PET findings, with pathologic correlations. Medicine (Baltimore) 2015;94(34):e1392
42 Zhang WD, Guan YB, Chen YF, Li CX. CT imaging of primary pleuropulmonary synovial sarcoma. Clin Radiol 2012;67(09):884–888
43 Baheti AD, Sewatkar R, Hornick JL, et al. Imaging features of primary and recurrent intrathoracic synovial sarcoma: a single-institute experience. Clin Imaging 2015;39(05):803–808

